Global Behavior of the Diffusion Coefficient for the Van der Waals Binary Mixture[1]

R. Castillo,[2] **M. E. Costas,**[2,3] **and A. Robledo**[2]

We describe the general dependence of the diffusion coefficient associated with the Van der Waals binary mixture on the temperature, number densities, and relative strengths of molecular interaction parameters. The task is facilitated by the fact that for Kac-type intermolecular potentials, in the long-range limit, the diffusion coefficient becomes simply related to the product of a partial compressibility and the curvature of the equilibrium free energy in the space of number densities. Therefore the different kinds of behavior found can be classified according to the scheme of Scott and Van Konynenburg for the global phase diagram of the same model mixture.

KEY WORDS: diffusion coefficient; free-energy curvature; mixtures; Van der Waals mixture.

1. INTRODUCTION

According to the familiar expressions of linear irreversible thermodynamics [1], the diffusion coefficient D for a binary mixture is a measure of a response to a chemical potential gradient. Therefore it can be expressed as the product of two terms, a mobility M and the second derivative of the system free-energy f with respect to composition x. Within such phenomenological theory the precise dependence of D on the reference or final equilibrium state and on the nature of the system is not readily obtainable. This is because details on the form of M and on the influence of the

compressible quality of the fluid (other than that implicit in d^2f/dx^2) are not given. Thus the usefulness of this simple and physically transparent expression appears limited in describing the dependence of D on temperature, density, composition, or intermolecular interaction parameters. The systematic study of the diffusion coefficient, with the capacity of broad comparison with experiment, would require, therefore, expressions obtained from statistical mechanical calculations on model systems.

A few years ago Karkheck et al. [2] derived an expression for the diffusion coefficient of the type described above for the Van der Waals fluid mixture model. In this expression, however, the form of the mobility M and the effect of the compressible quality of the mixture on D appear explicitly. They successfully applied a kinetic variational approach [3] based on maximization of entropy to a multicomponent system whose particles interact through a pair potential consisting of a hard core followed by an attractive tail of the Kac type [4]. As is well known [4], this interaction potential in its long-range limit leads to the familiar thermodynamic expressions for the Van der Waals fluid. It also conduces [5] to the interfacial density profiles and associated tensions for coexisting phases of the model mixture in a manner closely related to that prescribed by Van der Waals' theory of capillarity. When applied to transport properties, the Kac interaction in the long-range limit gives interesting results only for diffusion, mass or thermal; otherwise one obtains the transport coefficients that correspond only to the hard core [2, 6].

Another important modern development of the Van der Waals' theory of mixtures was the realization, following a more thorough investigation of its thermodynamic properties than during his own time [7], that the model mixture is capable of reproducing most known types of fluid–fluid phase equilibria observed in real mixtures. A readily accesible global phase diagram for a universe of binary mixtures is a valuable framework within which experimental information on many mixtures can be arranged and understood. An extension of the global phase diagram of the Van der Waals binary mixture to include interfacial properties, such as wetting properties, has also been performed [8]. The availability of a simple, closed-form expression for the diffusion constant of this model mixture suggests an exploration of its global behavior in parallel to the study of phase behavior. Here we present some results in the form of contours of equal value for this coefficient in the space of number densities at progressively higher temperatures for mixtures representative of each class in the Scott and Van Konynenburg classification [7].

2. THE DIFFUSION COEFFICIENT OF THE VAN DER WAALS MIXTURE

Notable among kinetic-equation approaches to the transport coefficients applicable to the liquid state is the mean-field variational theory of Karkheck and Stell [3]. Their development is an extension to interaction potentials with an attractive tail of the (improved [9]) kinetic theory of Enskog [10] for dense hard-sphere fluids. They incorporate this attractive tail into the kinetic equation in a mean-field linear term and succeed in retaining the analytical tractabililty and internal consistency (Onsager reciprocal equations and H-theorem) of the backgrownd hard-sphere problem. As expected for a mean-field approach, exact thermodynamic results are obtained for Kac-type potentials in the Van der Waals long-range limit. The scheme can be extended to a multicomponent system [2] and therefore to expressions for the transport coefficients of this well-known mixture model. These expressions are approximate [2] compared with those that result from other treatments [6] of the dynamics associated with the same Kac-type attractive potential. Nevertheless, they coincide in the Van der Waals infinitely weak and long-range limit in that only diffusion coefficients exhibit a dependence on the tail strength. In this limit viscosity and thermal conductivity coefficients coincide with those for a purely hard-core fluid [2, 6].

The expression for the (isothermal, isobaric, mass) diffusion coefficient D obtained from this approach has a remarkably simple and interesting form. For a mixture of two species, a and 2, and considering 2 as the solvent species, one has

$$D = \frac{n_1^2 n_2}{2n^2 k_B T} [d^{(1)} - d^{(2)}] \frac{\partial n_2}{\partial P} \left[\frac{\partial^2 f}{\partial n_1^2} \frac{\partial^2 f}{\partial n_2^2} - \left(\frac{\partial^2 f}{\partial n_1 \partial n_2} \right)^2 \right] \tag{1}$$

where n_1 and n_2 are the number densities, $n = n_1 + n_2$, P is the pressure, f is the Helmholtz free energy per unit volume, k_B is Boltzmann's constant, and T is the temperature. $d^{(1)}$ and $d^{(2)}$ are coefficients that appear in Sonine polynomial expansions of the one-particle distributions [2]. f has the form

$$f = k_B T \{ n_1 \ln n_1 + n_2 \ln n_2$$
$$+ (1 - \sigma_1 n_1 - \sigma_2 n_2) \ln(1 - \sigma_1 n_2) \ln(1 - \sigma_1 n_1 - \sigma_2 n_2) \}$$
$$- (a_{11} n_1^2 + 2a_{12} n_1 n_2 + a_{22} n^2) + f_0 \tag{2}$$

where σ_1 and σ_2 are the molecular diameters and a_{11}, a_{12}, and a_{22} are the interaction energy parameters. We have used a hard-rod representation for the hard-core contributions in order to obtain the familiar mixture model formulae.

Equation (1) can be seen to be composed of three factors, each with a clearly assignable meaning:

$$M = \frac{n_1^2 n_2}{2n^2 k_B T} [d^{(1)} - d^{(2)}] \qquad (3a)$$

$$K_2 = \frac{\partial n_2}{\partial P} \qquad (3b)$$

$$C = \frac{\partial^2 f}{\partial n_1^2} \frac{\partial^2 f}{\partial n_2^2} - \left(\frac{\partial^2 f}{\partial n_1 \partial n_2}\right)^2 \qquad (3c)$$

The first factor M is directly related to the dynamics of a two-particle collision and plays the role of the mobility in a phenomenological theory. The Sonine coefficients in M are determined by the hard-core interaction only, and their behavior can be extracted from the work of Kincaid et al. [11]. Basically, these coefficients are proportional to $(k_B T/n_1^2)^{1/2}$. The second factor K_2 is a partial compressibility. And the third factor is a measure of the curvature of the free energy f in the space of the number densities. The last two terms are easily determined for every given, one-phase, multiphase, or even metastable state (T, n_1, n_2) for all sets of interaction energy parameters, so that the global behavior of D for the Van der Waals mixture is directly accesible.

3. DIFFUSION COEFFICIENT BEHAVIOR FOR SOME REPRESENTATIVE MIXTURES

The global phase diagram for the Van der Waals mixture [7] is conveniently represented (when the core sizes of the two species are equal, $\sigma = \sigma_1 = \sigma_2$) in the space of the parameters

$$\zeta = (a_{22} - a_{11})/(a_{11} + a_{22}) \qquad (4a)$$

$$\Lambda = (a_{11} - 2a_{12} + a_{22})/(a_{11} + a_{22}) \qquad (4b)$$

where ζ is a measure of the difference in critical temperatures (or pressures) of the pure components and Λ is related to the heat of mixing at low temperatures. If the occurrence of azeothropy is not considered, five different regions can be distinghished in (ζ, Λ)-space. Systems with $\Lambda > 0$ exhibit three-phase coexistence lines that originate from $T = 0$ (classes [I, III, and IV). These three-phase states terminate at upper critical end points (UCEPs) of the liquid–liquid type for systems of class II. In class III triple points end at UCEPs of the liquid–gas type. Systems of type IV exhibit a second three-phase line at higher temperatures and therefore have two

UCEPs and one lower critical end point (LCEP). The two remaining types, I (with only liquid–gas coexistence) and V (with three-phase points bounded by one LCEP and one UCEP) occur for $\Lambda < 0$. There are additional interesting features in the global phase diagram, such as tricritical UCEPs in the symmetrical ($\zeta = 0$) type III mixtures and the so-called shield region that separates type II and type III mixtures along $\zeta = 0$; there, four-phase points connect four different triple-point lines.

The multiplicity of phases and the connectivity of their associated critical points are determined by the form that the spinodal surfaces [$C = 0$ in Eq. (2c)] display for every type of mixture. From Eq. (1) we note that D vanishes on these surfaces. In Fig. 1 we show contours of equal curvature C in the space of number densities at different temperatures for a symmetrical mixture of type II. (In Fig. 1 and in the subsequent figures we have taken $\sigma = 1$). As shown in Fig. 1, C increases steadily as the system is moved away from the spinodal surfaces and becomes infinite at the pure component boundaries and at close packing. The behavior of D is similar to that of C except that it is modulated by the compressibility K_2, which has the simple expression

$$K_2 = [kT(1 - \sigma n)^{-2} - 2a_{22}(n - \Lambda n_1)]^{-1} \tag{5}$$

All mixtures are incompressible at close packing, and the vanishing of K_2 there overwhelms the divergence of C, so that $D = 0$ when $\sigma n = 1$. In Fig. 2 we show contours of equal D (actually we calculate and show only $D_0 = D/M$ in what follows) for the same mixture of type II, where we observe the development of a saddle point in D_0 at temperatures beyond those at which the triple points terminate (Figs. 2b and c). As we see in other examples below, saddle points always arise in regions bounded by
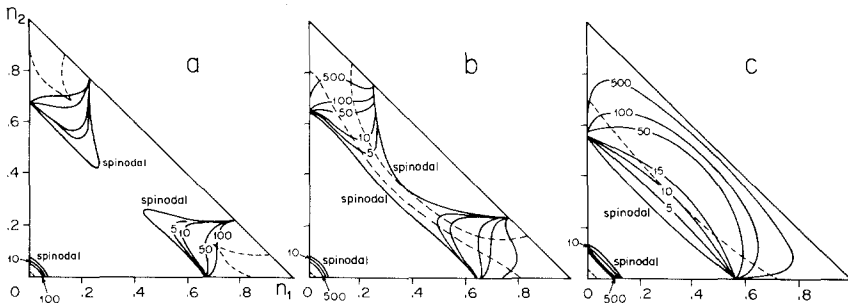

Fig. 1. Contours of equal curvature C for the free energy of a mixture of type II ($\zeta = 0$ and $\Lambda = 0.2$) in the space of number densities. (a) $T/T_C = 0.46$, (b) $T/T_C = 0.5$, and (c) $T/T_C = 0.7$, where T_C is the critical temperature of either pure component. σ is taken as unity and C is measured in units of $k_B T_C$. The dashed lines are the binodals.
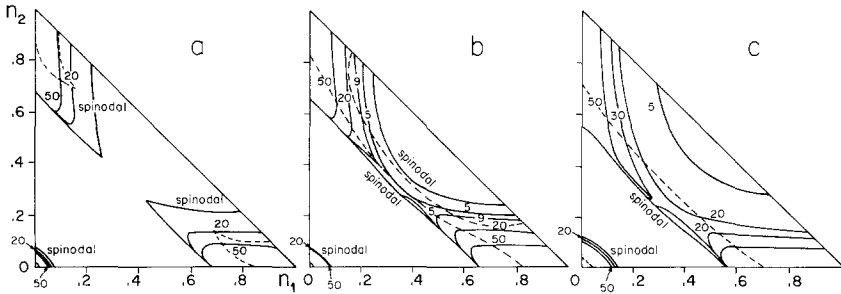
Fig. 2. Contours of equal value for the diffusion coefficient D_0 for the same mixture as in Fig. 1. (a) $T/T_C = 0.46$, (b) $T/T_C = 0.5$, and (c) $T/T_C = 0.7$. With our choice $\sigma = 1$, D_0 has no dimensions.

separate spinodal branches, or between close packing and a spinodal branch disconnected from it, provided $T > T_{UCEP}$. Another effect that K_2 has on D_0 is to impress some asymmetry over the otherwise symmetrical C countors in Fig. 1. The asymmetry is manifested as a shoulder close to the saddle point and adjacent to one of the liquid–gas spinodals in Figs. 2b and c. This shoulder arises from the term An_1 in Eq. (5), so that its location depends on the magnitude and sign on A. It is interesting to note, too, that the level curves for D_0 tend to become parallel to the triangle edges $(n_1, 0)$ and $(0, n_2)$ in the dense liquid region, and therefore D_0 remains practically constant under additions of the majoritary component but diminishes notably under additions of the minoritary component. The dashed lines in Fig. 2 are the binodals of the mixture; therefore some of the features that we have described correspond, at least for certain temperatures, to metastable states.

In Fig. 3 we show equal-level D_0 contours for a symmetrical mixture of type III. The main difference between this and the previous example is
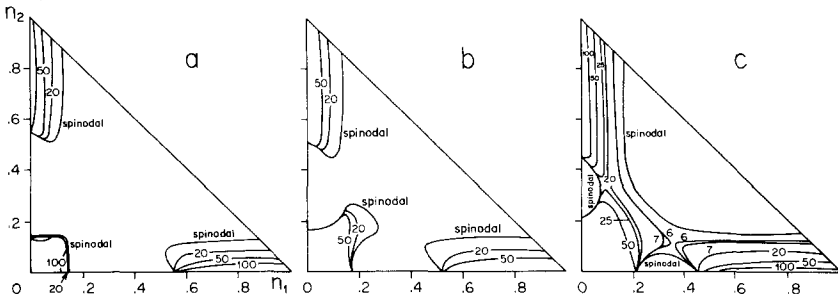
Fig. 3. Contours of equal value for the diffusion coefficient D_0 for a mixture of type III ($\zeta = 0$, $A = 0.5$). (a) $T/T_C = 0.735$, (b) $T/T_C = 0.8$, and (c) $T/T_C = 0.9$.

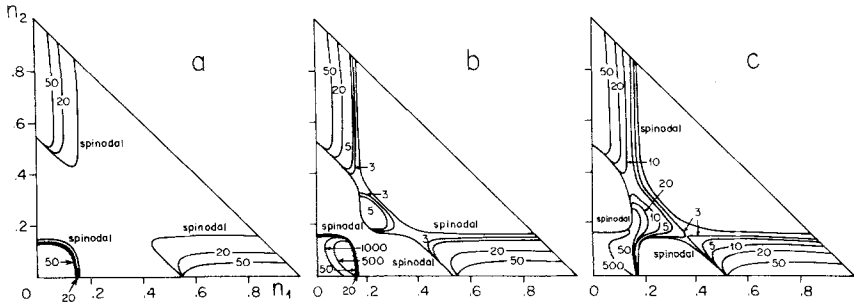**Fig. 4.** Contours of equal for the diffusion coefficient D_0 for a mixture in the shield region ($\zeta = 0$, $\Lambda = 0.42$). (a) $T/T_C = 0.75$, (b) $T/T_C = 0.775$, and (c) $T/T_C = 0.8$.

the existence of two saddle-point lines, which result from the development of two (instead of one) spinodal branches in the low-density region for temperatures above T_{UCEP}. Figure 4 shows our results for a symmetrical mixture on the shield region. The four-sphase point and the additional three-phase lines associated with this type of system make use of an island of stable states that exists within a finite range of temperatures in the middle of the (n_1, n_2)-triangle. This region is bounded by a spinodal surface that merges, as the temperature is raised, with the two spinodal branches located at the dense-liquid corners of the density triangle. Associated with this region we find a local maximum of D_0.

In Fig. 5a we show contours of D_0 for a nonsymmetric mixture of type III. And in Figs. 5b and c we show those found for a mixture of type IV at two different temperatures. Finally, in Fig., 6a we show contours of D_0 for a mixture of type I at two different temperatures, and in Fig. 6c those for a mixture of type V at a single temperature. An interesting feature observed in most of these examples is the occurrence of localized regions
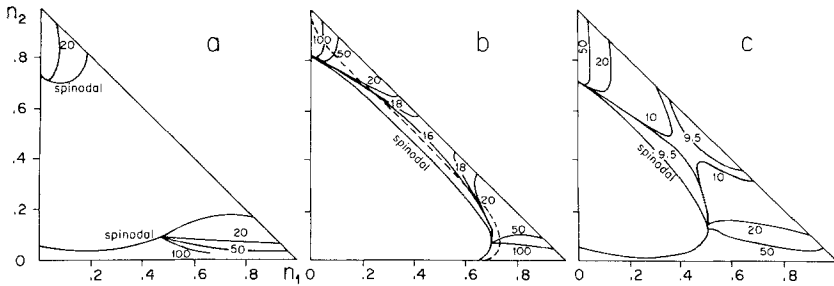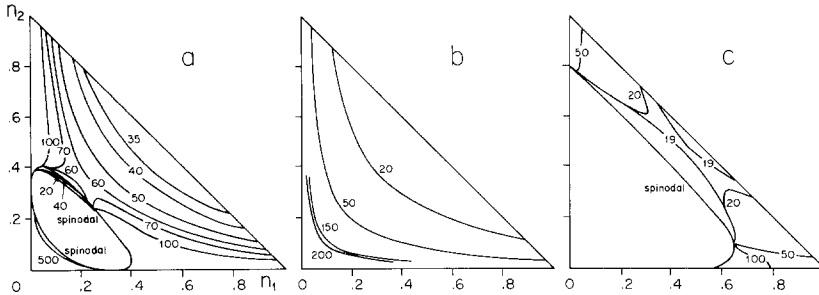

Fig. 5. Contours of equal value for the diffusion coefficient D_0 for (a) a mixture of type III ($\zeta = 0.6$, $\Lambda = 0.3$) at $T/T_C = 1.5$, (b) a mixture of type IV ($\zeta = 0.6$, $\Lambda = 0.01$) at $T/T_C = 0.7$, and (c) the same as but with $T/T_C = 1.5$. T_C is the critical temperature of the pure species 1.

Fig. 6. Contours of equal value for the diffusion coefficient D_0 for (a) a mixture of type 1 ($\zeta = 0$, $\Lambda = -0.33$) at $T/T_C = 1$, (b) the same as a but with $T/T_C = 2$, and (c) a mixture of type V ($\zeta = 0.8$, $\Lambda = -0.2$) with $T/T_C = 2$. T_C refers to the pure species 1.

in (n_1, n_2)-space, adjacent to the spinodal (in Figs. 5b and c and 6c where the spinodal bends), where the D_0 surface is very steep, and the coefficient experiences rapid changes with small variations in composition.

4. SUMMARY

We have explored the behavior that the diffusion coefficient in Eq. (1) generates when the full set of thermodynamic variables, including the particle interaction parameters, varies accross their physical range of values. A single expression describes both the gas and the dense-liquid regimes, and the pattens observed appear to be qualitatively correct. (i) The large values for D in the gas regions decrease steadily as the fluid becomes dense (Figs. 5a and 6b). (ii) The expected tendency, for the D_0 contours to become parallel to the triangle edges $(n_1, 0)$ and $(0, n_2)$ in the dense-liquid regions, was observed in all examples. Other features, such as the saddle points, might be observable in real mixtures. (The saddle point in Fig. 2b falls close to the liquid–vapor coexistence.) The rapid variations of D_0 that are found within the metastable regions imply strong effects on diffusion-driven growth of new-phase droplets formed by nucleation [12].

ACKNOWLEDGMENT

REFERENCES

1. See, for example, S. R. de Groot and P. Mazur, *Nonequilibrium Thermodynamics* (North-Holland, Amsterdam, 1969).
2. J. Karkheck, E. Martina, and G. Stell, *Phys. Rev.* **A25**:3328 (1982).
3. J. Karkheck and G. Stell, *J. Chem. Phys.* **75**:1475 (1981); *Phys. Rev.* **A25**:3302 (1982).
4. M. Kac, P. C. Hemmer, and G. E. Uhlenbeck, *J. Math. Phys.* **4**:216 (1963).
5. C. Varea, A. Valderrama, and A. Robledo, *J. Chem. Phys.* **73**:6255 (1980).
6. P. Resibois, J. Piasecki, and Y. Pomeau, *Phys. Rev. Lett.* **28**:882 (1972); M. Napiorkowski, J. Piasecki, M. Seghers, and P. Resibois, *J. Chem. Phys.* **66**:1422 (1977).
7. R. L. Scott and P. H. Van Konynenburg, *Discuss. Faraday Soc.* **49**:87 (1970); P. H. Van Konynenburg and R. L. Scott, *Philos. Trans. Soc. Lond. Ser. A* **298**:495 (1980).
8. M. E. Costas, C. Varea, and A. Robledo, *Phys. Rev. Lett.* **51**:2394 (1983).
9. H. van Beijeren and M. H. Ernst, *Physica* **68**:437 (1973); **70**:225 (1973).
10. See, for example, S. Chapman and T. G. Cowling, *The Mathematical Theory of Non-uniform Gases* (Cambridge University, New York, 1970).
11. J. M. Kincaid, M. Lopez de Haro, and E. G. D. Cohen, *J. Chem. Phys.* **79**:4505 (1983).
12. J. S. Langer and J. Schwartz, *Phys. Rev.* **A21**:949 (1980); see also C. M. Knobler, *Dynamics of Phase Transitions*, Notes for the 4th Mexican School on Statistical Mechanics (in press).